The genetic impact of an Ebola outbreak on a wild gorilla population

Claudia Fontsere[1*], Peter Frandsen[2,3*], Jessica Hernandez-Rodriguez[1], Jonas Niemann[4], Camilla Hjorth Scharff-Olsen[4], Dominique Vallet[5], Pascaline Le Gouar[5], Nelly Ménard[5], Arcadi Navarro[1,6,7], Hans R. Siegismund[2], Christina Hvilsom[3], M. Thomas P. Gilbert[4,8], Martin Kuhlwilm[1,†], David Hughes[1,9,10,†], Tomas Marques-Bonet[1,6,7,11,†]

[1]Institut de Biologia Evolutiva, (CSIC-Universitat Pompeu Fabra), PRBB, Doctor Aiguader 88, Barcelona, Catalonia 08003, Spain.
[2]Department of Biology, Section for Computational and RNA Biology, University of Copenhagen, Ole Maaløes Vej 5, 2200 Copenhagen, Denmark.
[3]Research and Conservation, Copenhagen Zoo, 2000 Frederiksberg, Denmark.
[4]Center for Evolutionary Hologenomics, The GLOBE Institute, University of Copenhagen, 1353 Copenhagen, Denmark
[5]UMR 6553, ECOBIO: Ecosystems, Biodiversity, Evolution, CNRS/University of Rennes 1, Station Biologique de Paimpont, 35380 Paimpont, France.
[6]CNAG-CRG, Centre for Genomic Regulation (CRG), Barcelona Institute of Science and Technology (BIST), Baldiri i Reixac 4, 08028 Barcelona, Spain.
[7]Institucio Catalana de Recerca i Estudis Avançats (ICREA), Barcelona, Catalonia 08010, Spain.
[8]University Museum, NTNU, Trondheim, Norway
[9]Population Health Sciences, Bristol Medical School, University of Bristol, Bristol, UK.
[10]MRC Integrative Epidemiology Unit at University of Bristol, Bristol, UK
[11]Institut Català de Paleontologia Miquel Crusafont, Universitat Autònoma de Barcelona, Edifici ICTA-ICP, c/ Columnes s/n, 08193 Cerdanyola del Vallès, Barcelona, Spain

* These authors contributed equally to this work

† These authors share co-last authorship.

Authors for correspondence: Claudia Fontsere (claudia.fontsere@upf.edu), Tomas Marques (tomas.marques@upf.edu), Martin Kuhlwilm (martin.kuhlwilm@upf.edu)

Abstract

Background

Numerous Ebola virus outbreaks have occurred in Equatorial Africa over the past decades. Besides human fatalities, gorillas and chimpanzees have also succumbed to the fatal virus. The 2004 outbreak at the Odzala-Kokoua National Park (Republic of Congo) alone caused a severe decline in the resident western lowland gorilla (*Gorilla gorilla gorilla*) population, with a 95% mortality rate. Here, we explore the immediate genetic impact of the Ebola outbreak in the western lowland gorilla population.

Results

Associations with survivorship were evaluated by utilizing DNA obtained from fecal samples from 16 gorilla individuals declared missing after the outbreak (non-survivors) and 15 individuals observed before and after the epidemic (survivors). We used a target enrichment approach to capture the sequences of 123 genes previously associated with immunology and Ebola virus resistance and additionally analyzed the gut microbiome which could influence the survival after an infection. Our results indicate no changes in the population genetic diversity before and after the Ebola outbreak, and no significant differences in microbial community composition between survivors and non-survivors. However, and despite the low power for an association analysis, we do detect six nominally significant missense mutations in four genes that might be candidate variants associated with an increased chance of survival.

Conclusion

This study offers the first insight to the genetics of a wild great ape population before and after an Ebola outbreak using target capture experiments from fecal samples, and presents a list of candidate loci that may have facilitated their survival.

Keywords

Ebola; gorilla; non-invasive samples; candidate genes

Background

The Ebola virus (EBOV), discovered in 1976, causes a severe disease and often fatal hemorrhagic fever for which numerous human outbreaks have been reported throughout Africa [1]. The most virulent outbreak reported to date was in West Africa in December 2013 and lasted until 2016 with more than 28,000 confirmed or suspected human cases and more than 11,000 human deaths [2]. Since then, other outbreaks of Ebola have been observed. In June 2020, when the 2018 outbreak was declared over by the World Health Organization (WHO), 3,470 cases had been reported with 2,287 deaths (fatality rate of 66%) [3].

EBOV belongs to the single-stranded RNA virus family *Filoviridae* [4] with five distinct strains in the Ebola genus: *Zaire*, *Sudan*, *Budibugyo*, *Taï Forest* and *Reston*. The first three are responsible for the majority of human infections [5, 6]. The virus is highly infectious and can enter the body through direct contact of broken skin or mucous membranes with infected blood or body fluids, causing symptoms including fever, vomiting, diarrhea, internal and external bleeding. Ebola hemorrhagic fever or Ebola virus disease (EVD) is an acute and severe disease with a fatality rate in humans around 50% [5–7].

Infectious diseases such as Ebola are considered to be a threat to the survival of African great apes [8], together with other threats such as habitat loss, climate change and poaching [9]. In some cases, the human outbreaks have been linked to contact with infected bushmeat from gorillas or chimpanzees [10] and several surveys have reported dramatic declines in populations of great apes in parallel with human EVD outbreaks with laboratory confirmation of Ebola virus infection in some carcasses [10–12]. Gorilla populations from the Republic of Congo suffered severe die-offs during a chuman EVD outbreak near the Lossi sanctuary in 2002-2003 [12] and Odzala-Kokoua National Park in 2004 [13] with reported mortality rates as high as

95%. In Lossi sanctuary alone, it was estimated that the Ebola virus killed 5,000 wild gorillas [12]. The severe population decline has contributed to the 2007 shift of the conservation status of western gorillas from “endangered” to “critically endangered” by the International Union for Conservation of Nature (IUCN) [14]. Furthermore, the recent outbreak of human EVD in North Kivu (Democratic Republic Congo) [3] was in close proximity to the remnant populations of eastern gorilla species, hence a human to ape transmission of the virus could potentially mark the end of existence for this critically endangered species.

Threats such as infectious diseases are relevant for conservation efforts, and efficient strategies are needed to reduce the effects of EVD on wild great ape populations [15]. Understanding any genetic impact that EBOV outbreaks might have on wild populations is vital, as EVD contributes to the fragmentation of gorilla populations due to a heterogeneous spatial influence of the outbreak [16]. Social dynamics in gorillas are rapidly affected by Ebola through a decrease in social cohesion, although recovery after the outbreak has been observed [17, 18]. One study reported that solitary individuals were less affected than individuals living in groups, marking the relevance of social dynamics for transmission [13]. A previous study using 17 microsatellites found no loss of genetic diversity after one EBOV outbreak in Lossi sanctuary and Odzala-Kokoua National Park, which could be explained by post-epidemic immigration, sufficiently large remnant effective population size or a short period of time after the decline [18]. The present study represents a continuation of this aforementioned research since many aspects of EBOV infection in wild gorilla populations are not yet explored, such as genetic variants in survivors that might contribute to resistance or higher chance of survival to EVD. In humans, such an approach was used during the 2014 EBOV outbreak, although no evidence of adaptation was found in the survivors [19].

Furthermore, microbial organisms inhabiting the gut also play a potentially crucial role in training and maintaining the immune system [20–22]. Where some commensal microbes are associated with priming the immune response or activating antiviral responses, others facilitate

104 the development of the infection or suppress the immune response [23]. For instance, a recent
105 study reported a link between the gastrointestinal microbiome of healthy humans and a
106 predisposition to severe COVID-19 [24], with an abundance of Klebsiella, Streptococcus, and
107 Ruminococcus being correlated with elevated levels of proinflammatory cytokine. The
108 association between infectious diseases and the gut microbiome of nonhuman primates is less
109 well understood. While the gut microbiome of SIVgor-infected (gorilla Simian
110 Immunodeficiency virus) wild gorillas seems to be more robust to dysbiosis than those of
111 chimpanzees and humans [25], it is unclear how shifts in the gorilla gut microbiome can impact
112 the severity of viral infections, and in particular the immune response to Ebola virus infection.

113 Long-term monitoring of a western lowland gorilla (*Gorilla gorilla gorilla*) population in
114 Odzala-Kokoua National Park (Republic of Congo) has been ongoing since 2001 until 2017
115 encompassing the Ebola outbreak of 2004 [16–18, 26] which resulted in a mortality rate of 95%
116 [13]. Population monitoring involved the recording of individual histories of hundreds of
117 identified individuals, the determination of sex, age and social status and the collection of fecal
118 samples in different time periods. This close monitoring through time was fundamental to
119 determine which individuals were either not affected or survived the Ebola outbreak and which
120 went missing with their cause of death assumed to be EVD.

121 Here, we have obtained genetic data from gorilla fecal samples pre- and post-outbreak
122 to explore potential associations to survivorship. Particularly, we compare the genetic variation
123 at the single nucleotide level in 123 autosomal target-captured genes with putative roles in
124 virus immune response and the gut microbiome composition in a reduced panel of survivors
125 and non-survivors of this Zaire EBOV outbreak. With that we show that targeted capture on
126 non-invasive fecal samples and next-generation sequencing can be used to study the impact
127 of this severe disease in a natural population.

Results

A total of 31 non-invasive fecal samples from identified western lowland gorillas were collected between 2001 and 2014 in Odzala-Kokoua National Park, Congo [18] (Fig. 1A). Sixteen of these were from individuals declared missing after the Zaire Ebola virus outbreak in 2004, and suspected to have died because of the infection, here termed 'non-survivors'. These samples were collected between 2001 and 2004. The remaining 15 samples were from gorillas identified before the epidemic and still observed after the epidemic, and will be identified henceforth as 'survivors' [17]. These 15 samples were collected between 2005 and 2014 (Supplementary Table S1). We used target capture enrichment to sequence the genomic regions of 123 genes, which had previous evidence of putative roles in immune response to EBOV or other viruses (Supplementary Table S2). In addition, 15 neutral regions previously studied in other human and non-human primate studies were also targeted [27, 28] (Supplementary Table S2). Target design and all analyses were performed using the human reference genome due to the higher quality of annotations compared to the gorilla reference genome. We sequenced an average of 73 million paired reads per individual, 12% of which were unique (Supplementary Table S3). On average, 0.38% of the data mapped to the target space, representing an on-target effective coverage of 53.89-fold (range: 2.52-fold to 230.70-fold; Fig. 1B, Supplementary Table S3), with 72% of the target space covered by at least 4 reads per individual. Samples G282, G1392 and G638 performed poorly, with <50% of the target space covered at a minimum depth of 4 reads (Supplementary Fig. S1). Overall performance can be assessed by calculating how well the capture resequencing experiment went relative to expectations had we performed random shotgun sequencing. In that regard, we observe an average enrichment of 125-fold (88 - 346-fold) (Supplementary Table S3). Individuals with extremely low proportions of target space covered by at least 4 reads (<30%) (G638 and G282) and high heterozygosity and high levels of human contamination were

153 removed from further analysis (individuals G374 and G1392, Fig. 1C and Supplementary Fig.
154 S2, Table S3).

155 With the final dataset of 13 survivors and 14 non-survivors, we validated that the
156 genotype information obtained was in concordance with previously published gorilla whole-
157 genomes, as determined by a principal component analysis (PCA) (Supplementary Fig. S3).
158 We estimated kinship for each pair of individuals, identifying a single case of close relatedness
159 (1st degree) among them (non-survivor G374 and survivor G739; kinship coefficient = 0.4)
160 (Supplementary Fig. S4). In addition, we observed no stratification correlating with
161 survivor/non-survivor classification. Individuals appear to be dispersed randomly across a
162 dendrogram derived from shared genotype likelihood dosage states (Fig. 2A), and a univariate
163 linear regression of survivorship on the top 5 PCs identified no significant structure associated
164 to survivorship (P-value > 0.1; Supplementary Fig. S5). Hence, we determined no genome-
165 wide group structure differences between survivors and non-survivors. The overall level of
166 genetic diversity within the target space of the studied gorillas was, on average, lower than that
167 of western lowland gorillas obtained from whole-genome sequencing (Supplementary Fig. S6)
168 [29, 30], an expected outcome following the target capture procedure. Moreover, there are no
169 statistically significant differences in heterozygosity between survivors and non-survivors
170 (Student's t-test, p-value=0.34; Fig. 2B).

171 In order to determine genetic differences between the groups, we calculated three
172 summary statistics on a dataset of 6,852 high-quality variants: (1) the difference in allele
173 frequency (ΔFrequency), (2) the fixation index (F_{ST}), and (3) the significance level (α) of each
174 variant for its association with the binary trait survivor/non-survivor (Fig. 3). We found 118 SNPs
175 within the target space that surpassed our α threshold in the association test, and we also
176 reported their ΔFrequency and F_{ST} values. However, after controlling for type I error none of
177 these remained significant. Out of these, seven genes have multiple nominally significant SNPs
178 (*CD1B, IGKV4-1, HLA-A, ACTB, LYN, CD68* and *MX1*), while 10 neutral regions (~10kb each)

have at least 1 nominally significant variant (Supplementary Table S4). For comparative validation, we repeated the association analysis using ANGSD [31], a software explicitly built to work with low coverage data that relies on genotype likelihoods. With this method, we were able to recover the majority of the genes found above (30 out of 36). However, ANGSD returned more hits and thus more genes (Supplementary Figs. S7, S8 and Table S5), rendering the above approach more conservative.

Next, we explored the potential functional impact of the variants in the nominally significant candidate loci that differentiate survivors from non-survivors. While we found no significant associations with gene ontology categories, the analysis of predictions of functional consequences pinpointed six missense mutations which differed in frequency between the two groups (Supplementary Table S6), one each in the *ATM, IGKV4-1* and *RNF167* genes (all lower in survivors) and three in the *ACTB* (Actin Beta) gene (one unique to survivors, two lower in survivors, Supplementary Table S4). All three missense variants in *ACTB* are predicted as deleterious by both the PolyPhen [32] and SIFT [33] algorithms. Furthermore, the derived variant in survivors in the immunoglobuline-encoding *IGKV4-1* might be deleterious (C-score > 20 [34]), hence potentially functionally relevant. Since we used the human genome for target design, mapping and variant calling, we caution that differences in exon usage or pseudogenization on the gorilla lineage might confound these inferences of protein-coding changes. In order to confirm the expression of these genes, and specifically the exons of interest, we mapped transcriptome data from six tissues in gorillas [35] to the same reference genome, and quantified expression levels. We confirmed the expression of these genes and found high transcript abundance (log2-value of counts >=9) for *ACTB*, *RNF167* and *ATM*, while *IGKV4-1* was only detected at low levels in these tissues (log2-value of counts = 5.84). We found ~10,000 RNA sequencing reads overlapping the three loci of interest in *ACTB*, 437 in *RNF167*, and 96 in *IGKV4-1*, supporting the expression of these specific loci in gorilla tissues, while for *ATM* only 10 reads overlapped (Supplementary Table S6).

Among the 118 significant SNPs, we found no direct overlap with loci associated to 2,385 traits in genome-wide association studies (GWAS) for humans [36]. However, we found 49 associated loci within close proximity (5,000 bp) to GWAS loci (Supplementary Table S7), among which the locus 19:1104078 near GPX4 stands out for its association with five blood cell traits (counts and percentages of leukocyte cell types). Furthermore, 6:29916885 in the *HLA* is associated to hemoglobin levels. Five loci in *HLA-DRA* are associated with different autoimmune diseases like systemic lupus erythematosus or multiple sclerosis (Supplementary Table S7). Furthermore, nine loci in this region (*HLA-DRB5* and *HLA-A*) are associated with schizophrenia or autism spectrum disorder (Supplementary Table S7).

It has been reported that intestinal microbiota play a critical role in immune response to infectious diseases [20–22]. Thus, the microbiome might be relevant for the survival of wild gorilla populations experiencing an Ebola outbreak. Taking advantage of the nature of the samples, we first analyzed the microbiota present in each fecal extraction using a 16S rRNA library (Methods). We obtained a total of 96,928,400 reads with an average sequencing depth of 1,101,459 (SD ± 418,989) reads per gorilla fecal extraction (Supplementary Table S8), and determined the abundance of taxa (Supplementary Figs. S9 and S10). Firmicutes (53.79%), Bacteroidetes (12.02%) and Chloroflexi (11.11%) were the predominant phyla (Supplementary Fig. S9 and Table S9), that include the following most abundant orders: Clostridiales (39.37%), Bacillales (11.24%), Bacteroidales (10.87%) and Anaerolineales (11.11%) (Supplementary Fig. S10 and Table S10), concordant with previous findings [37, 38]. We found no taxa significantly differing in relative abundance between survivor and non-survivor gorillas (Bonferroni-corrected p-values > 0.05; Supplementary Fig. S11 and Table S11), and sample groups were not separated in a clustering analysis (Fig. S12).

Since these results on the gut microbiome diversity did not support differences between both gorilla groups, we decided to perform deep sequencing on the fecal libraries. We generated a total of 801,132,281 sequences from DNA libraries (4,025,054-25,593,317

231 reads per sample; Supplementary Table S8) and used MALT (MEGAN Alignment Tool) [39] for
232 an alternative characterization of the microbial profile of the samples (Supplementary Fig. S13).
233 We find that the majority of the identified taxa are associated with the gut microbiome
234 (Supplementary Table S12 and S13). By far the most abundant taxon is the gut bacterium
235 *Escherichia coli*, which could be detected in all samples, and makes up more than 50% of all
236 assigned sequences in nine of the samples. Also in high abundance are species of the
237 Bacteroidales order, such as *Bacteroides cellulosilyticus* and *Prevotella spp.*, as well as
238 members of the Clostridiales, Lactobacillales, and Bacillales orders, corroborating previous
239 reports on the composition of western lowland gorilla gut microbiomes [40, 41]. Furthermore,
240 we detected pathogenic taxa in high abundance in some of the samples, such as *Clostridium*
241 *botulinum*, *Acinetobacter baumannii*, and *Klebsiella pneumoniae*, which have been previously
242 found in the gorilla gut [42]. However, the microbial profiles of survivors and non-survivors do
243 not differ significantly from each other in this analysis either (Bonferroni-corrected p-values >
244 0.05, two-sided t-test, Supplementary Table S11), and the two groups do not form separate
245 clusters in a Principal Coordinate analysis or a Neighbor Joining Tree (Supplementary Figs.
246 S14 and S15).

247

248 # Discussion

249 We investigated non-invasive fecal samples from a long-term monitored population of
250 western lowland gorillas in the Republic of Congo, including individuals that most likely
251 succumbed to the *Zaire* Ebola virus outbreak in 2004, as well as surviving individuals [17, 18].
252 We used targeted capture of 123 autosomal genes with putative roles in immune response to
253 EBOV or other viruses (Supplementary Table S2) from fecal samples. This yielded an
254 enrichment of more than 100-fold across samples, and a medium to high coverage of the target
255 space across most individuals (Supplementary Fig. S1 and Table S3). Although a large
256 proportion of reads were duplicates, the overall performance was high and these results

257 demonstrate the great potential of capture experiments for obtaining genotypes from fecal
258 samples of wild great ape populations [43, 44], for which high-coverage sequencing would be
259 prohibitively expensive. We determined that the studied individuals were not closely related,
260 hence most likely representing a random sampling of the wild gorilla population before and
261 after the outbreak. We also investigated the microbial community composition of survivors and
262 non-survivors, finding no significant differences in taxa abundance, neither using 16S rRNA or
263 deep sequencing data (Supplementary Figs. S11, S13 and Table S11). Hence, we find no
264 evidence that the gut microbiome of individuals has an influence on the survival rate of wild
265 gorillas exposed to Ebola. However, these observations are limited by (1) the sample size, and
266 (2) the broad range of collection dates (Supplementary Table 1). The latter is particularly true
267 (2a) relative to the timing of any exposure, but also in respect to the (2b) dynamic nature of the
268 gut microbiome [38].

269 Given the limited sample size, we developed an approach using differences in allele
270 frequency, the fixation index and the effect size to determine variants most strongly associated
271 to survivability in the studied population, generally replicable using an association analysis with
272 ANGSD. While 44 of the 118 nominally significant SNPs (Supplementary Table S4) do fall within
273 10 of the 15 neutral regions included in the study, some SNPs might be functionally relevant
274 for surviving the EBOV outbreak. The non-synonymous variants in *ACTB*, *RNF167* and *IGKV4-*
275 *1* genes are obvious candidate loci, and particularly the three deleterious missense mutations
276 in Actin Beta appear to be strong candidates for a higher survival rate. The actin cytoskeleton
277 is important for virus assembly [45], and a disturbed assembly process could have influenced
278 the viral load in individuals with changes in this protein. As expected for a gene encoding a
279 structural protein, *ACTB* is highly expressed in gorilla tissues. Furthermore, the variant in
280 *IGKV4-1* might improve the immune response to viral infection through antigen recognition
281 [46]. The missense mutation in ATM, which belongs to the PI3-kinase family, could interfere

with the cellular entry specifically of the Ebola virus [47], although we could not confirm expression of this locus *in vivo* in the available tissues.

We find other potentially relevant non-coding variants, 49 of which are in close proximity to SNPs associated to GWAS traits in humans, suggesting possible regulatory functions (Supplementary Table S7). Among those, the association of *GPX4* with leukocyte cell type count might reflect differences in leukocyte composition after viral infection. Differences in hematocrit or hemoglobin levels might have contributed to the survival of wild gorillas considering that hemorrhage and internal bleeding are symptoms of Ebola infection. Since eight loci are associated to the *HLA-DRB* gene, a direct involvement in the adaptive immune system might cause the signature observed at this locus, particularly given that human survivors of EVD show a lower frequency of *HLA-DR*-positive T cells [48].

Conclusion

By using fecal samples and targeted capture enrichment, non-invasive assessment of numerous individuals from wild populations is possible. Here, we demonstrate that this approach can be used to analyze temporal genetic changes in wild great ape populations in response to environmental factors. Additionally, we present candidate loci that may have facilitated the survival of gorilla individuals or groups after an outbreak of the *Zaire* Ebola virus. Understanding putative adaptive responses to this pathogen in wild populations can help to advance our knowledge on the natural dynamics of this severe disease. Such a strategy might be useful in a broader context, since these and other primates are susceptible to other infectious diseases such as Covid-19 [49].

Methods

Samples, DNA extraction, library preparation. Non-invasive fecal samples from western lowland gorillas were collected between 2001 and 2014 in Odzala-Kokoua National

Park, Republic of Congo [18]. Among them, we selected 31 samples from previously identified individuals. Sixteen of those individuals were declared missing after the epidemic in 2004 [13]. They died during the time span of the epidemic and were identified here as non-survivors. Fifteen individuals were observed before and after the epidemic, and were described here as survivors (Fig. 1A and Supplementary Table S1) [17]. Samples were collected by field investigators wearing masks and gloves, and were dried with silica beads and then stored at room temperature until arrival in a laboratory where they were stored at 4°C until extraction.

DNA was extracted from 10mg of dried sample using the 2CTAB/PCI protocol [50] using negative controls that were checked for contamination before subsequent experiment. Three different extractions were carried out, except for samples G778, G374, G344, G498 and G372, where only two extractions were performed (Supplementary Table S1). A DNA library [51–53] and a 16S rRNA library [54–56] were prepared for each extract. Isolated DNA samples were quantified with Qubit with a mean estimated concentration of 13.3 ng/µl (range: 0.90-74.7). Whenever possible, a total of 250 ng of DNA was used to construct DNA libraries, but never more than a total volume of 33 µl was taken from any single sample. DNA was sheared with a Covaris S2 instrument and 88 fecal DNA (fDNA) libraries were prepared following a custom dual-indexing protocol with 25 cycles of amplification [51, 52]. Subsequent to DNA library preparation, 88 16S rRNA libraries were prepared using 1 µl of total DNA. The V3 and V4 regions of 16S rRNA were target amplified using modified 341F and 806Rb primers [54, 55, 57], incorporated into the dual-indexing protocol [52]. The forward primer (IS1_P5_16S_341f: ACACTCTTTCCCTACACGACGCTCTTCCGATCTNNNNCCTACGGGNGGCWGCAG), and reverse primer (IS2_P7_16S_806rB: GTGACTGGAGTTCAGACGTGTGCTCTTCCGATCTGGACTACNVGGGTWTCTAAT) include the complementary sequences necessary for the final indexing step [52]. Protocols are provided in [53].

Target Design, Capture and Sequencing. RNA baits covering the target space were designed and synthesized by Agilent with a minimum of 3x bait coverage. The target space included specific autosomal genes (123 genes) and 15 neutral regions (~10kb each) (Supplementary Table S2). For target enrichment, the fDNA libraries were pooled into one equimolar batch and subjected to two consecutive rounds of DNA capture with the RNA baits in 8 hybridizations. Captured fDNA libraries were sequenced on the Illumina system in four HiSeq 2500 2x125 lanes and one HiSeq 2500 rapid run at 2x250 bp. The 16S libraries were sequenced on one HiSeq 2500 rapid run 2x250 bp lane. In addition, we generated paired-end sequences from the fDNA libraries on four HiSeq 4000 lanes (2x150bp) to study the whole microbiome composition (Table S8).

Mapping and Variant Discovery. Prior to mapping, paired-end reads belonging to the same library but sequenced in different lanes were merged into a single FASTQ file. PCR duplicates were directly removed from FASTQ files using FASTuniq (v1.1) [58]. Overlapping reads were merged (minimum overlap of 10 bp, minimum length of final read to 50 bp) using PEAR (v0.9.6) [59]. Reads were mapped using BWA mem (v0.7.12) [60] to the human reference genome Hg19 (GRCh37 from the UCSC database). Assembled reads were mapped considering single-end specifications and unassembled reads considering paired-end specifications. Any remaining PCR duplicates were removed using PicardTools MarkDuplicates (v1.95) (http://broadinstitute.github.io/picard/). Non-primary alignments and reads with quality below 30 were filtered from the dataset with samtools (v1.5) [61]. Finally, single-end and paired-end reads were merged into a single BAM file using PicardTools MergeSamFiles (http://broadinstitute.github.io/picard/). The percentage of aligned reads for each DNA extraction and sample was calculated by dividing the number of uniquely and high-quality mapped reads (without duplicates) by the total number of sequenced reads. The percentage of on-target aligned reads was calculated for each sample by dividing the number of on-target filtered reads by the number of sequenced reads. The average target effective

coverage was calculated dividing the number of aligned bases by the total length of the targeted genomic space. Finally, the enrichment factor (ER) of the capture performance was calculated using the ratio between the on-target reads by the total mapped reads over the targeted size by genomic size (ER = (On-Target Reads/Mapped Reads)/(Target Size/Genome Size)). The coverage for each target region was retrieved using SAMtools bedcov [61].

For variant calling, all BAM files belonging to the same sample were merged into a single BAM file using PicardTools MergeSamFiles (v1.95) (http://broadinstitute.github.io/picard/). Variant discovery was performed using GATK 'Unified Genotyper' [62] for each sample independently with the following parameters -out_mode EMIT_ALL_SITES -stand_call_conf 5.0 -stand_emit_conf 5.0 -A BaseCounts -A GCContent -A RMSMappingQuality -A BaseQualityRankSumTest. Afterwards, we merged each sample gvcf to a single one using GATK `CombineVariants' [62] with the following parameters -genotypeMergeOptions UNIQUIFY –excludeNonVariant. We also included in the gvcf the genotype information of available whole genome data of six *Gorilla beringei beringei*, eight *Gorilla beringei graueri*, one *Gorilla gorilla dielhi*, and twenty-three *Gorilla gorilla gorilla* samples [29, 30]. The VCF was filtered with VCFtools [63] to keep only biallelic positions with DP >3 and quality > 30 and without indels.

Genotype likelihoods were directly obtained from BAM files with ANGSD [31] including four *Gorilla beringei beringei*, four *Gorilla beringei graueri*, one *Gorilla gorilla dielhi*, and four *Gorilla gorilla gorilla*, with the following parameters and only in the target space: -uniqueOnly 1 -remove_bads 1 -only_proper_pairs 1 -trim 0 -C 50 -baq 1 -minInd 21 -skipTriallelic 1 -GL 2 -minMapQ 30 -doGlf 2 -doMajorMinor 1 -doMaf 2 -minMaf 0.05 -SNP_pval 1e-6.

Quality control. We evaluated the amount of human contamination in each fecal library using the HuConTest script [64], as described previously [65]. The majority of samples have less than 2% of human contamination, but samples G348 and G1392 have estimates of human

383 contamination of 6.7% and 25.1%, respectively (Supplementary Table S3). These two samples
384 also show extreme values of heterozygosity (deviating >1s.d. from mean heterozygosity; Figure
385 S2). For the identification of individuals and markers with elevated missing data rates we used
386 the proportion of the target space covered by at least 4 reads. Individuals with less than 30%
387 of covered target space (4 reads) were not used for further analysis (G638 and G282).

388 A principal component analysis (PCA) was performed to validate that the genotype
389 information obtained for the case study gorillas was in concordance with previously published
390 data. We used PCAngsd [66] with the genotype likelihoods obtained with ANGSD (N=6,484),
391 including 13 previously published whole-genomes representative of each know gorilla
392 subspecies [29, 30]. We also obtained a PCA using the GATK genotype calls after keeping only
393 variants with minor allele frequency of 0.02 with plink --pca option (N=6051) [67].

394 **Genetic distance, relatedness and heterozygosity.** We used the genotype likelihood
395 information for the studied individuals to obtain the genetic distance by running ngsDist in
396 ANGSD [68] with the following parameters: --n_sites 5477 --probs TRUE --pairwise_del. Then,
397 we constructed an Euclidean distance matrix based on the genotypes and performed a
398 hierarchical clustering using the R package *ape* [69]. We also run PCAngsd [66] considering
399 only the study gorillas to discard any possible intra-group structure.

400 The theta coefficients of kinship (probability of a pair of randomly sampled homologous
401 alleles are identical by descent) were calculated using the NgsrelateV2 [70, 71] on the
402 genotype likelihood obtained with ANGSD [31]. Note that all possible genotype likelihoods,
403 even outside the target space (N=226,094), were used since the coverage of the kinship
404 markers was insufficient.

405 To assess global levels of heterozygosity, the unfolded SFS was calculated for each
406 sample separately, including thirteen gorilla whole-genomes representative of all gorilla
407 subspecies [29, 30], using ANGSD [31] and realSFS [72] only in the target space with the

following quality filter parameters: -uniqueOnly 1 -remove_bads 1 -only_proper_pairs 1 -trim 0 -C 50 -baq 1 -minMapQ 20 -minQ 20 -setMaxDepth 200 -doCounts 1 -GL 1 -doSaf 1. We used the human genome (Hg19) to determine the ancestral state.

Association analysis. The genotype calls obtained with GATK were further filtered with Plink [67] to exclude variants considering their missing rate (--geno 0.05), minor allele frequency (--maf 0.01) and Hardy-Weinberg equilibrium (--hwe 0.00001). The final dataset consists of 27 samples (13 survivors and 14 non-survivors) and 6,852 high-quality variants. Nominal significance was set at an alpha of 0.05 and a Bonferroni corrected alpha threshold of 7.3x10-6 (0.05/6,852) was defined to account for familywise error. Associations were tested for by a chi-square allelic test with one degree of freedom and p-values were estimated by permutation in plink (plink –assoc –mperm 10000). [73]. The p-values were plotted in a Manhattan plot in R (v3.4.1).

The allele frequency for each group (survivors and non-survivors) was obtained using the -freq2 option in VCFtools [63]. Then, we calculated the allele frequency difference per SNP by subtracting the allele frequency in non-survivors from the allele frequency in survivors (ΔFrequency). We chose a threshold of ± 0.2, and plotted the allele frequencies using R. The fixation index (F_{ST}) between both groups was calculated using VCFtools –weir-fst-pop option (Weir and Cockerham) [63] with a threshold at 0.15, and results were plotted in R. We retrieved markers with $\alpha \leq 0.05$ in the association test and a p-value < 0.05 in the permutation test. The ANGSD software [31] was used to perform a replication of the association analysis using the following parameters -minQ 20 -minMapQ 30 -doAsso 1 -GL 1 -out assocGQ_filter -doMajorMinor 1 -doMaf 1 -SNP_pval 1e-6 -minInd 22 -minMaf 0.02. The output of the association analysis are LRT values (Likelihood Ratio Test), which are chi square distributed with one degree of freedom. Since we set a threshold of significance at 95% confidence, the minimum score to be significant is LRT = 3.84. In both association analyses, we linked the nominally significant SNPs with their genes (Supplementary Table S4 and S5). Genes with

multiple nominally significant SNPs were considered to be potentially more relevant. Subsequently, we compared the overlap of discovered genes between the datasets (Unified Genotyper and ANGSD) in a Venn diagram (Supplementary Fig. S8) using the R package VennDiagram [74].

Prediction of functional consequences of the significant markers. We used VEP (v91) [75] for the functional annotation of the associated SNPs. We retrieved the predicted consequence of each significant marker found in the potentially related genes to Ebola immune response, as well as PolyPhen-2 [32], Sift [76] and C-scores [77]. Associated loci were intersected with hits in the GWAS catalogue [78] within 5,000 bp. We also performed an overrepresentation test using Panther [79] to test whether any of the potentially related genes are overrepresented in biological or functional categories compared to the rest of targeted genes with no apparent association with Ebola. In addition, we mapped previously published RNA sequencing data from six tissues (brain, cerebellum, heart, kidney, liver, testis) in two gorilla individuals [35] to the annotated genes in the human reference genome (using the Ensembl Release 75 gene models) using Tophat2 [80], and estimated the gene expression with htseq-count [81]. Gene expression is reported log2-normalized, and we counted the number of reads overlapping the candidate missense mutations to confirm their transcriptional activity in gorillas. Values presented are the cumulative sums of RNA sequencing reads across individuals and tissues.

Microbiome sequencing. 16S RNA sequencing reads were processed using QIIME (v1) (Quantitative Insights Into Microbial Ecology) [82] to analyze the 16S rRNA. First, paired-end raw reads were merged using fastq-join from ea-utils package [83]. Then, with usearch software [84], merged FASTQ reads were filtered (-fastq_trunclen 253 and –fastq_maxee 0.5). Using QIIME environment, the metadata mapping file was constructed and validated (validate_mapping_file.py) and QIIME labels were added (add_qiime_labels.py). We applied open-reference OTUs picking (pick_open_reference_otus.py). Summary statistics were

460 computed using *biom summarize-table*. The resulting dataset was rarefied to an even depth of
461 10,000 sequences per extract (6 extracts were excluded in diversity analysis: G191_5782,
462 G344_5827, G314_5824, G489_5834, G489_5835, G344_5828). Finally, we ran diversity
463 analysis with a sequence depth of 10,000 (core_diversity_analysis.py). Taxa abundance
464 quantification and significance or relative taxa abundance (T-test and p-values adjusted for
465 multiple testing with Bonferroni-correction) were computed in R.

466 Deep sequencing of the DNA library (pre-capture) was performed as stated above. To
467 remove sequencing adapters and merge the read pairs, we used AdapterRemoval v2.2.4 with
468 default settings [85]. We then aligned the merged sequences to the gorilla reference genome
469 Kamilah_GGO_v0 using bwa mem [60] to remove host DNA. Subsequently we filtered out
470 potential human contaminant DNA by aligning the unmapped sequences to the human
471 reference genome hg19, resulting in 724,738,878 filtered sequences. MALT v0.4.1 (MEGAN
472 Alignment Tool) [39] was used to characterize the microbial profile, using all archaeal, viral,
473 and bacterial reference sequences downloaded from NCBI on 06.05.2019. These were
474 indexed using malt-build to build a custom database. Malt-run was then used with minimum
475 percent identity (--minPercentIdentity) set to 95, the minimum support (--minSupport)
476 parameter set to 10, and the top percent value (--topPercent) set as 1, other parameters were
477 set to default. The resulting rma6 files were visualized with MEGAN6 [86] and clustered in a
478 Principal Coordinate analysis (PCoA) and Neighbor Joining Tree analysis according to
479 microbial composition on the species level (Supplementary Figs. S14 and S15).

480

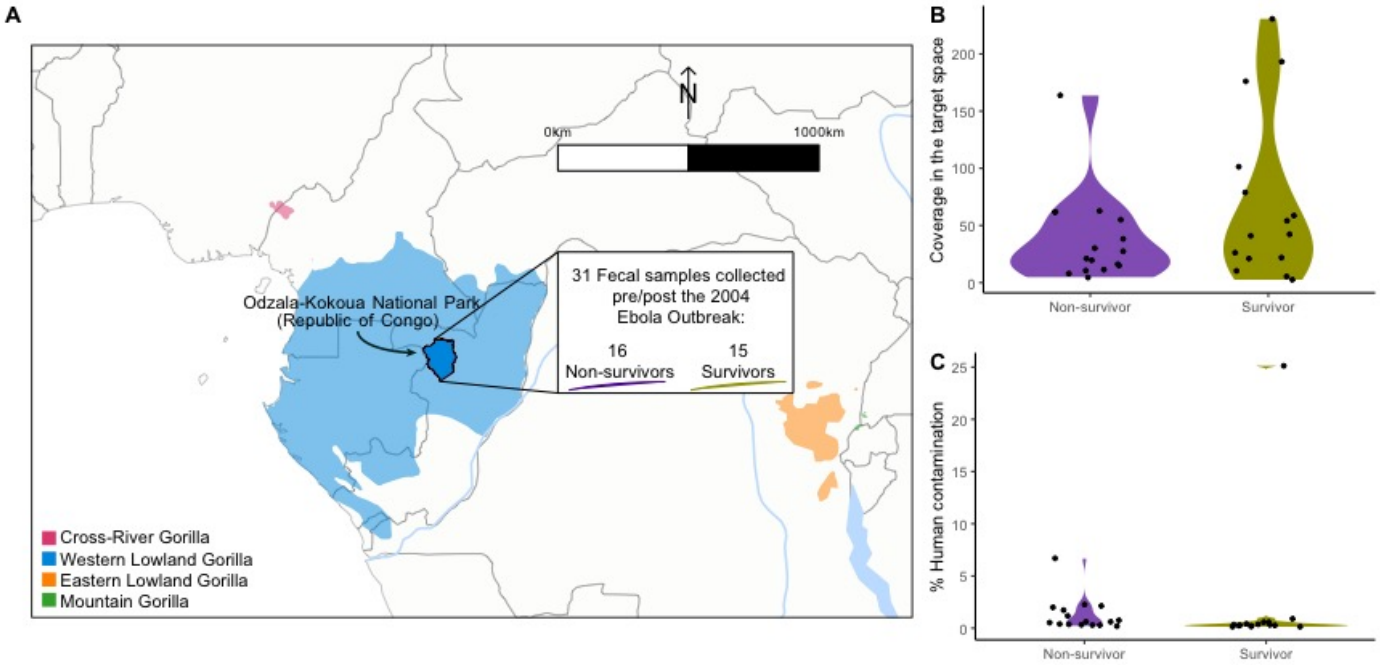

481

482 **Fig. 1**. **Sample description. A**) Geographical map of the extant range of gorillas and the
483 Odzala-Kokoua National Park (Republic of Congo) where fecal samples were collected
484 between 2001 and 2014, overlapping the Ebola outbreak in 2004. **B**) Average coverage
485 reached in the target space per sample in both studied groups. **C**) Percentage of human
486 contamination in each fecal sample.

487

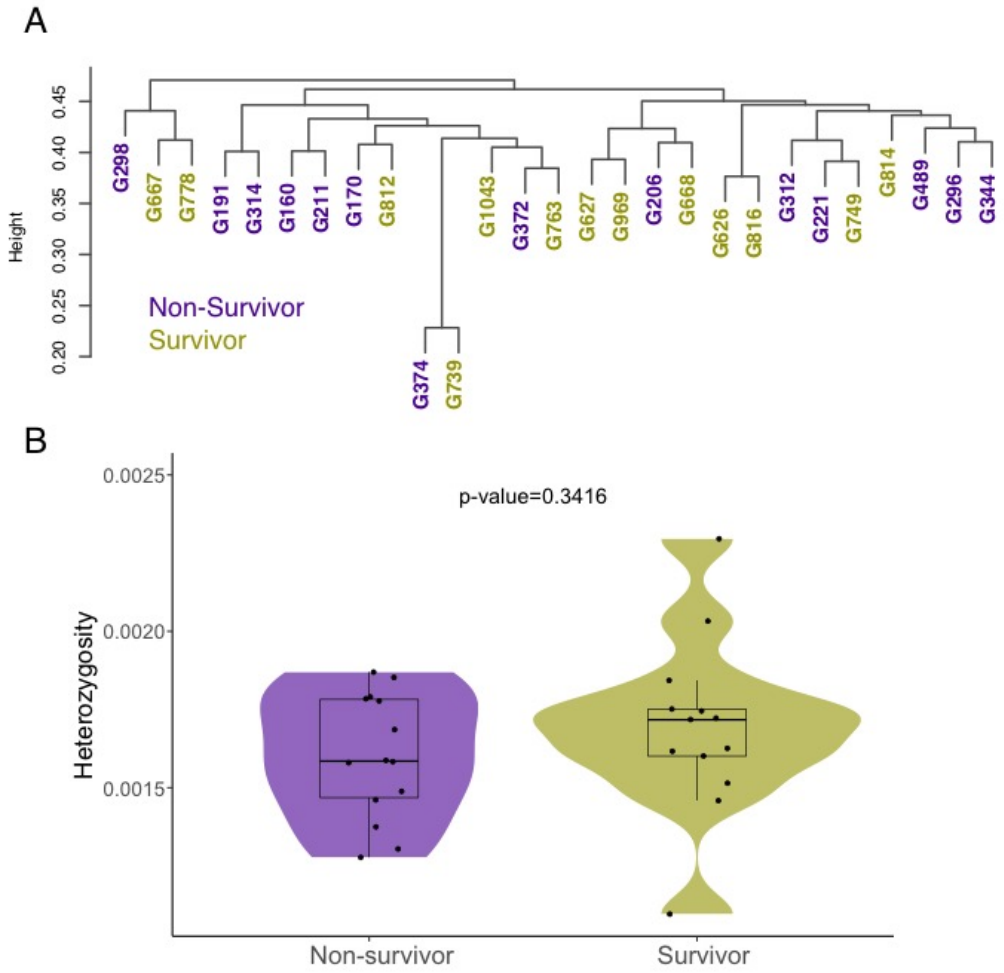

Fig. 2. Genetic distance dendrogram and heterozygosity among non-survivor and survivor gorilla groups. A) Clustering dendrogram of pairwise genetic distance derived from genotype likelihoods (N=5,477). **B)** Mean heterozygosity (bp^{-1}) in non-survivors and survivors; not significantly different (Student t-test, p-value=0.34).

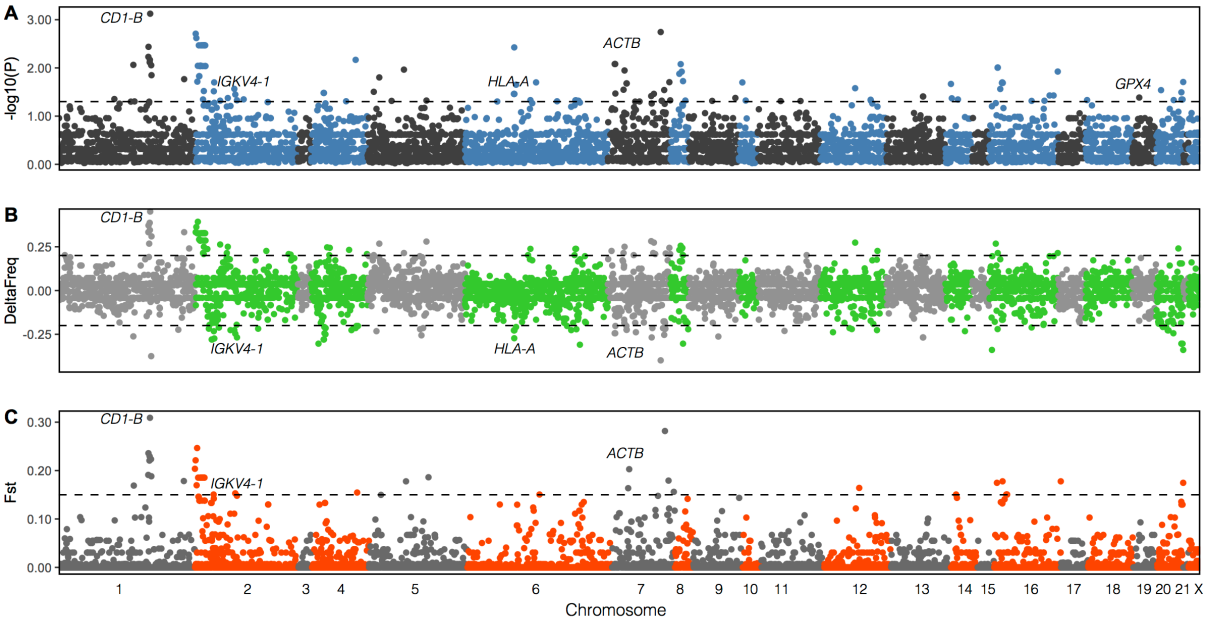

495

496 **Fig. 3. Association analysis to detect SNPs and candidate genes related to survivorship**
497 **to EBOV outbreak. A)** Significance level (threshold set at α=0.05, -log10(P-value)=1.30). **B)**
498 Difference in allele frequency (threshold set at ±0.2). **C)** Fixation index (threshold set at
499 F_{ST}=0.15). Dashed lines delineate the thresholds used.

Availability of data and materials

The dataset generated during the current study will be made publicly available upon acceptance (raw sequencing data to ENA, project ID: PRJEB43265). It will be available to reviewers from the corresponding author on request.

Abbreviations

EBOV: Ebola virus

EVD: Ebola virus Disease

GWAS: Genome-Wide Association Study

IUCN: International Union for Conservation of Nature

PCA: Principal Component Analysis

SNP: Single Nucleotide Polymorphism

References

1. Centers for Disease Control and Prevention. History of Ebola Virus Disease. U.S. Department of Health & Human Services. 2018.

2. World Health Organization. Situation Report - Ebola Virus Disease. 2016.

3. World Health Organization. External Situation Report 98 - Ebola Virus Disease. 2020. https://www.who.int/publications/i/item/10665-332654.

4. Kuhn JH, Becker S, Geisbert TW, Johnson KM, Kawaoka Y, Lipkin WI, et al. Proposal for a revised taxonomy of the family Filoviridae: classification, names of taxa and viruses, and virus abbreviations. 2010;155:2083–103.

5. Centers of Disease Control and Prevention. What is Ebola Virus Disease? 2018.

6. World Health Organization. Ebola virus disease. 2018.

7. Feldmann H. Ebola haemorrhagic fever. Lancet. 2011;377:849–62.

8. Smith KF, Acevedo-Whitehouse K, Pedersen AB. The role of infectious diseases in biological conservation. Anim Conserv. 2009;12:1–12.

9. Walsh PD, Abernethy KA, Bermejo M, Beyers R, De Wachter P, Akou ME, et al. Letters To Nature. Nature. 2003;422 April:611–4.

10. Rouquet P, Froment J-M, Bermejo M, Kilbourn A, Karesh W, Reed P, et al. Wild Animal Mortality Monitoring and Human Ebola Outbreaks, Gabon and Republic of Congo, 2001–2003. Emerg Infect Dis. 2005;11:283–90.

11. Leroy EM, Rouquet P, Formenty P, Kilbourne A, Froment J, Bermejo M, et al. Mulitple Ebola Virus Transmission Events and Rapid Decline of Central African Wildlife. Science (80-). 2004;303 January:387–90.

12. Bermejo M, Rodríguez-teijeiro JD, Illera G, Barroso A, Vilà C, Walsh PD. Ebola Outbreak Killed 5000 Gorillas. 2006;314 December.

13. Caillaud D, Levréro F, Cristescu R, Gatti S, Dewas M, Douadi M, et al. Gorilla susceptibility to Ebola virus: the cost of sociality. Curr Biol. 2006;16:489–91.
14. Maisels F, Bergl R, Williamson E. Gorilla gorilla (errata version published in 2016). The IUCN Red List of Threatened Species. 2016.
15. Leendertz SAJ, Wich SA, Ancrenaz M, Bergl RA, Gonder MK, Humle T, et al. Ebola in great apes – current knowledge, possibilities for vaccination, and implications for conservation and human health. Mamm Rev. 2017;47:98–111.
16. Genton C, Cristescu R, Gatti S, Levréro F, Bigot E, Motsch P, et al. Using demographic characteristics of populations to detect spatial fragmentation following suspected ebola outbreaks in great apes. Am J Phys Anthropol. 2017;164:3–10.
17. Genton C, Cristescu R, Gatti S, Levréro F, Bigot E, Caillaud D, et al. Recovery Potential of a Western Lowland Gorilla Population following a Major Ebola Outbreak: Results from a Ten Year Study. PLoS One. 2012;7:e37106.
18. Le Gouar PJ, Vallet D, David L, Bermejo M, Gatti S, Levréro F, et al. How Ebola impacts genetics of Western lowland gorilla populations. PLoS One. 2009;4:e8375.
19. Li X, Zai J, Liu H, Feng Y, Li F, Wei J, et al. The 2014 Ebola virus outbreak in West Africa highlights no evidence of rapid evolution or adaptation to humans. Nat Publ Gr. 2016; June:1–9.
20. Honda K, Littman DR. The microbiome in infectious disease and inflammation. Annu Rev Immunol. 2012;30:759–95.
21. Fiebiger U, Bereswill S, Heimesaat MM. Dissecting the interplay between intestinal microbiota and host immunity in health and disease: Lessons learned from germfree and gnotobiotic animal models. Eur J Microbiol Immunol. 2016;6:253–71.
22. Zheng D, Liwinski T, Elinav E. Interaction between microbiota and immunity in health and disease. Cell Res. 2020;30:492–506.
23. Domínguez-Díaz C, García-Orozco A, Riera-Leal A, Padilla-Arellano JR, Fafutis-Morris M. Microbiota and its role on viral evasion: Is it with us or against us? Front Cell Infect Microbiol. 2019;9 JUL:256.
24. Gou W, Fu Y, Yue L, Chen GD, Cai X, Shuai M, et al. Gut microbiota may underlie the predisposition of healthy individuals to COVID-19. medRxiv. 2020.
25. Moeller AH, Peeters M, Ayouba A, Ngole EM, Esteban A, Hahn BH, et al. Stability of the gorilla microbiome despite simian immunodeficiency virus infection. Mol Ecol. 2015;24:690–7.
26. Genton C, Pierre A, Cristescu R, Lévréro F, Gatti S, Pierre J-S, et al. How Ebola impacts social dynamics in gorillas: a multistate modelling approach. J Anim Ecol. 2015;84:166–76.
27. Fischer A, Prüfer K, Good JM, Halbwax M, Wiebe V, André C, et al. Bonobos fall within the genomic variation of Chimpanzees. PLoS One. 2011;6:1–10.
28. Voight BF, Adams AM, Frisse LA, Qian Y, Hudson RR, Di Rienzo A. Interrogating multiple aspects of variation in a full resequencing data set to infer human population size changes. Proc Natl Acad Sci U S A. 2005;102:18508–13.
29. Prado-Martinez J, Sudmant PH, Kidd JM, Li H, Kelley JL, Lorente-Galdos B, et al. Great ape genetic diversity and population history. Nature. 2013;499:471–5. doi:10.1038/nature12228.
30. Xue Y, Prado-martinez J, Sudmant PH, Narasimhan V, Ayub Q, Szpak M, et al. Mountain gorilla genomes reveal the impact of long-term population decline and inbreeding. Science (80-). 2015;348:242–5.
31. Korneliussen TS, Albrechtsen A, Nielsen R. ANGSD: Analysis of Next Generation Sequencing Data. BMC Bioinformatics. 2014.
32. Adzhubei IA, Schmidt S, Peshkin L, Ramensky VE, Gerasimova A, Bork P, et al. A method and server for predicting damaging missense mutations. Nat Methods. 2010;7:248–9.
33. Vaser R, Adusumalli S, Leng SN, Sikic M, Ng PC. SIFT missense predictions for

587 genomes. Nat Protoc. 2016;11:1–9.
588 34. Kircher M, Witten DM, Jain P, O'roak BJ, Cooper GM, Shendure J. A general
589 framework for estimating the relative pathogenicity of human genetic variants. Nat Genet.
590 2014;46:310–5.
591 35. Brawand D, Soumillon M, Necsulea A, Julien P, Csárdi G, Harrigan P, et al. The
592 evolution of gene expression levels in mammalian organs. Nature. 2011;478.
593 36. MacArthur J, Bowler E, Cerezo M, Gil L, Hall P, Hastings E, et al. The new NHGRI-
594 EBI Catalog of published genome-wide association studies (GWAS Catalog). Nucleic Acids
595 Res. 2017;45 Database issue:D896–901. doi:10.1093/nar/gkw1133.
596 37. Gomez A, Petrzelkova K, Yeoman CJ, Vlckova K, Koppova I, Carbonero F, et al. Gut
597 microbiome composition and metabolomic profiles of wild western lowland gorillas (Gorilla
598 gorilla gorilla) reflect host ecology. 2015; September 2014:2551–65.
599 38. Hicks AL, Lee KJ, Couto-Rodriguez M, Patel J, Sinha R, Guo C, et al. Gut
600 microbiomes of wild great apes fluctuate seasonally in response to diet. Nat Commun.
601 2018;9:1786.
602 39. Vågene ÅJ, Herbig A, Campana MG, Robles García NM, Warinner C, Sabin S, et al.
603 Salmonella enterica genomes from victims of a major sixteenth-century epidemic in Mexico.
604 Nat Ecol Evol. 2018;2:520–8. doi:10.1038/s41559-017-0446-6.
605 40. Gomez A, Rothman JM, Petrzelkova K, Yeoman CJ, Vlckova K, Umaña JD, et al.
606 Temporal variation selects for diet–microbe co-metabolic traits in the gut of Gorilla spp. ISME
607 J. 2016;10:514–26. doi:10.1038/ismej.2015.146.
608 41. Gomez A, Petrzelkova K, Yeoman CJ, Vlckova K, Mrázek J, Koppova I, et al. Gut
609 microbiome composition and metabolomic profiles of wild western lowland gorillas (Gorilla
610 gorilla gorilla) reflect host ecology. Mol Ecol. 2015;24:2551–65.
611 42. Bittar F, Keita MB, Lagier J-C, Peeters M, Delaporte E, Raoult D. Gorilla gorilla gorilla
612 gut: a potential reservoir of pathogenic bacteria as revealed using culturomics and molecular
613 tools. Sci Rep. 2014;4:7174. doi:10.1038/srep07174.
614 43. Hernandez-Rodriguez J, Arandjelovic M, Lester J, de Filippo C, Weihmann A, Meyer
615 M, et al. The impact of endogenous content, replicates and pooling on genome capture from
616 faecal samples. Mol Ecol Resour. 2017. doi:10.1111/1755-0998.12728.
617 44. Fontsere C, Alvarez-Estape M, Lester J, Arandjelovic M, Kuhlwilm M, Dieguez P, et
618 al. Maximizing the acquisition of unique reads in non-invasive capture sequencing experiments.
619 Mol Ecol Resour. 2020;n/a n/a. doi:https://doi.org/10.1111/1755-0998.13300.
620 45. Kerviel A, Thomas A, Chaloin L, Favard C, Muriaux D. Virus assembly and plasma
621 membrane domains: Which came first? Virus Res. 2013;171:332–40.
622 46. Lefranc M-P. Immunoglobulin and T Cell Receptor Genes: IMGT® and the Birth and
623 Rise of Immunoinformatics. Front Immunol. 2014;5:22.
624 47. Saeed MF, Kolokoltsov AA, Freiberg AN, Holbrook MR, Davey RA.
625 Phosphoinositide-3 Kinase-Akt Pathway Controls Cellular Entry of Ebola Virus. PLoS Pathog.
626 2008;4:e1000141.
627 48. Ruibal P, Oestereich L, Lüdtke A, Becker-Ziaja B, Wozniak DM, Kerber R, et al.
628 Unique human immune signature of Ebola virus disease in Guinea. Nat 2016 5337601.
629 2016;533:100.
630 49. Melin AD, Janiak MC, Marrone F, Arora PS, Higham JP. Comparative ACE2 variation
631 and primate COVID-19 risk. Commun Biol. 2020;3:641. doi:10.1038/s42003-020-01370-w.
632 50. Vallet D, Petit EJ, Gatti S, Levréro F, Ménard N. A new 2CTAB/PCI method improves
633 DNA amplification success from faeces of Mediterranean (Barbary macaques) and tropical
634 (lowland gorillas) primates. Conserv Genet. 2008;9:677–80.
635 51. Meyer M, Kircher M. Illumina Sequencing Library Preparation for Highly Multiplexed
636 Target Capture and Sequencing. Cold Spring Harb Protoc. 2010;2010:pdb.prot5448-
637 pdb.prot5448.
638 52. Kircher M, Sawyer S, Meyer M. Double indexing overcomes inaccuracies in

multiplex sequencing on the Illumina platform. Nucleic Acids Res. 2012;40.

53. Rohland N, Reich D. Cost-effective, high-throughput DNA sequencing libraries for multiplexed target capture. Genome Res. 2012;22:939–46.

54. Hugerth LW, Wefer HA, Lundin S, Jakobsson HE, Lindberg M, Rodin S, et al. DegePrime, a program for degenerate primer design for broad-taxonomic-range PCR in microbial ecology studies. Appl Environ Microbiol. 2014;80:5116–23.

55. Klindworth A, Pruesse E, Schweer T, Peplies J, Quast C, Horn M, et al. Evaluation of general 16S ribosomal RNA gene PCR primers for classical and next-generation sequencing-based diversity studies. Nucleic Acids Res. 2013;41:e1–e1.

56. Caporaso JG, Lauber CL, Walters WA, Berg-Lyons D, Huntley J, Fierer N, et al. Ultra-high-throughput microbial community analysis on the Illumina HiSeq and MiSeq platforms. ISME J. 2012;6:1621–4.

57. Caporaso JG, Lauber CL, Walters WA, Berg-Lyons D, Huntley J, Fierer N, et al. Ultra-high-throughput microbial community analysis on the Illumina HiSeq and MiSeq platforms. ISME J. 2012;6:1621–4.

58. Xu H, Luo X, Qian J, Pang X, Song J, Qian G, et al. FastUniq: A Fast De Novo Duplicates Removal Tool for Paired Short Reads. PLoS One. 2012;7:1–6.

59. Stamatakis A, Zhang J, Kobert K. Genome analysis PEAR : a fast and accurate Illumina Paired-End reAd mergeR. 2014;30:614–20.

60. Li H, Durbin R. Fast and accurate short read alignment with Burrows-Wheeler transform. Bioinformatics. 2009;25:1754–60.

61. Li H, Handsaker B, Wysoker A, Fennell T, Ruan J, Homer N, et al. The Sequence Alignment/Map format and SAMtools. Bioinformatics. 2009;25:2078–9.

62. Depristo MA, Banks E, Poplin R, Garimella K V, Maguire JR, Hartl C, et al. A framework for variation discovery and genotyping using next-generation DNA sequencing data. Nat Genet. 2011;43:491–8.

63. Danecek P, Auton A, Abecasis G, Albers CA, Banks E, DePristo MA, et al. The variant call format and VCFtools. Bioinformatics. 2011;27:2156–8.

64. Kuhlwilm M, Fontsere C, Han S, Alvarez-Estape M, Marques-Bonet T. HuConTest: Testing human contamination in great ape samples. Genome Biology and Evolution. 2021; doi: 10.1093/gbe/evab117.

65. Fontsere C, Alvarez-Estape M, Lester J, Arandjelovic M, Kuhlwilm M, Dieguez P, et al. Maximizing the acquisition of unique reads in non-invasive capture sequencing experiments. Mol Ecol Resour. 2020;:1755-0998.13300.

66. Meisner J, Albrechtsen A. Inferring population structure and admixture proportions in low-depth NGS data. Genetics. 2018;210:719–31.

67. Purcell S, Neale B, Todd-Brown K, Thomas L, Ferreira MAR, Bender D, et al. PLINK: A tool set for whole-genome association and population-based linkage analyses. Am J Hum Genet. 2007;81:559–75.

68. Vieira FG, Lassalle F, Korneliussen TS, Fumagalli M. Improving the estimation of genetic distances from Next-Generation Sequencing data. Biol J Linn Soc. 2016;117:139–49. doi:https://doi.org/10.1111/bij.12511.

69. Paradis E, Claude J, Strimmer K. APE: Analyses of phylogenetics and evolution in R language. Bioinformatics. 2004;20:289–90.

70. Korneliussen TS, Moltke I. NgsRelate: A software tool for estimating pairwise relatedness from next-generation sequencing data. Bioinformatics. 2015;31:4009–11.

71. Hanghøj K, Moltke I, Andersen PA, Manica A, Korneliussen TS. Fast and accurate relatedness estimation from high-throughput sequencing data in the presence of inbreeding. Gigascience. 2019;8.

72. Nielsen R, Korneliussen T, Albrechtsen A, Li Y, Wang J. SNP calling, genotype calling, and sample allele frequency estimation from new-generation sequencing data. PLoS One. 2012;7.

691 73. Purcell S, Neale B, Todd-Brown K, Thomas L, Ferreira MAR, Bender D, et al. PLINK:
692 A tool set for whole-genome association and population-based linkage analyses. Am J Hum
693 Genet. 2007;81:559–75.
694 74. Chen H, Boutros PC. VennDiagram: a package for the generation of highly-
695 customizable Venn and Euler diagrams in R. 2011.
696 75. McLaren W, Gil L, Hunt SE, Riat HS, Ritchie GRS, Thormann A, et al. The Ensembl
697 Variant Effect Predictor. Genome Biol. 2016;17:122. doi:10.1186/s13059-016-0974-4.
698 76. Sim N, Kumar P, Hu J, Henikoff S, Schneider G, Ng PC. SIFT web server : predicting
699 effects of amino acid substitutions on proteins. 2012;40 June:452–7.
700 77. Kircher M, Witten DM, Jain P, O'Roak BJ, Cooper GM, Shendure J. A general
701 framework for estimating the relative pathogenicity of human genetic variants. Nat Genet.
702 2014;46:310–5.
703 78. Macarthur J, Bowler E, Cerezo M, Gil L, Hall P, Hastings E, et al. The new NHGRI-
704 EBI Catalog of published genome-wide association studies (GWAS Catalog). 2017;45
705 November 2016:896–901.
706 79. Thomas PD, Campbell MJ, Kejariwal A, Mi H, Karlak B, Daverman R, et al.
707 PANTHER : A Library of Protein Families and Subfamilies Indexed by Function. Genome Res.
708 2003;:2129–41.
709 80. Kim D, Pertea G, Trapnell C, Pimentel H, Kelley R, Salzberg SL. TopHat2: accurate
710 alignment of transcriptomes in the presence of insertions, deletions and gene fusions. Genome
711 Biol. 2013;14:R36. doi:10.1186/gb-2013-14-4-r36.
712 81. Anders S, Pyl PT, Huber W. HTSeq--a Python framework to work with high-
713 throughput sequencing data. Bioinformatics. 2015;31:166–9.
714 82. Caporaso JG, Kuczynski J, Stombaugh J, Bittinger K, Bushman FD, Costello EK, et
715 al. QIIME allows analysis of high- throughput community sequencing data. Nat Methods.
716 2010;7:335–6.
717 83. Aronesty E. ea-utils : "Command-line tools for processing biological sequencing
718 data." 2011.
719 84. Edgar RC. Search and clustering orders of magnitude faster than BLAST.
720 Bioinformatics. 2017;26:2460–1.
721 85. Schubert M, Lindgreen S, Orlando L. AdapterRemoval v2: rapid adapter trimming,
722 identification, and read merging. BMC Res Notes. 2016;9:88. doi:10.1186/s13104-016-1900-2.
723 86. Huson DH, Auch AF, Qi J, Schuster SC. MEGAN analysis of metagenomic data.
724 Genome Res . 2007;17:377–86. doi:10.1101/gr.5969107.
725

726 Declarations

727 Acknowledgments

728 We are grateful to S. Gatti, F. Levréro, C. Genton, R. Cristescu for their assistance with
729 sample collection on site. We thank the teams of the ECOFAC program (EU) and African Parks
730 Networks for logistic assistance and permission to work in Odzala-Kokoua National Park. The
731 storage and extraction of fecal samples were performed in the molecular ecology platform
732 (UMR 6553 Ecobio, CNRS/UR1) dedicated to non-invasive samples.

Funding

C.F. is supported by “la Caixa” PhD fellowship, fellowship code LCF/BQ/DE15/10360006. M.K. is supported by “la Caixa” Foundation (ID 100010434), fellowship code LCF/BQ/PR19/11700002. J.N is supported by the European Union's Horizon 2020 research and innovation programme under grant agreement no. 676154 (ArchSci2020) and an EMBO short-term fellowship STF-8036. P.F. is supported by the Innovation Fund Denmark. H.R.S is supported by The Danish Council for Independent Research | Natural Sciences. A.N. is supported by BFU2015-68649-P (MINECO/FEDER, UE). M.T.P.G. is supported by the Danish Basic Research Foundation award DNRF143. T.M.-B is supported by BFU2017-86471-P (MINECO/FEDER, UE), U01 MH106874 grant, Howard Hughes International Early Career, Obra Social "La Caixa" and Secretaria d’Universitats i Recerca del Departament d’Economia i Coneixement de la Generalitat de Catalunya. P.L.G., N.M. and D.V. are supported by the French National agency for research via the ANR-11-JVS7–015 IDiPop project. D.H. is supported by Wellcome Investigator Award (202802/Z/16/Z) and works in the Medical Research Council Integrative Epidemiology Unit at the University of Bristol, which is supported by the Medical Research Council (MC_UU_00011/1-7). This long-term research on gorillas was funded by the ECOsystèmes FORestiers program (Ministère de l’Ecologie et du Développement Durable France), the Espèces-Phares program (DG Environnement, UE) and Lundbeck Foundation Visiting Professorship R317-2019-5 grant to T.M.-B. and M.T.P.G.

Contributions

D.H., T.M.-B., P.L.G., N.M., D.V., A.N. and M.T.P.G. conceived and designed the study; D.H., D.V. and C.S.O. performed experiments; C.F., M.K., D.H., J.H.R., C.H.S.O and J.N. analyzed data; P.L.G., N.M. and D.V. collected genetic and demographic data; P.F., H.R.S., C.H., provided analytical support. C.F., M.K., D.H., and T.M.-B. wrote the manuscript with input and approval from the other authors.

Corresponding authors

Correspondence to: Claudia Fontsere (claudia.fontsere@upf.edu), Tomas Marques-Bonet (tomas.marques@upf.edu) or Martin Kuhlwilm (martin.kuhlwilm@upf.edu)

Ethics declarations

Ethics approval and consent to participate

Not applicable.

Consent for publication

Not applicable.

Competing interests

The authors declare that they have no competing interests.

Additional information

Additional File 1. Excel file with tables S1-S13.

Additional File 2. PDF with Figures S1-S15.